

Synthetic Diagnostic Approach to Analysis of Imaging Bolometer Data from LHD

B. J. Peterson¹, K. Mukai¹, S. Pandya², R. Sano², M. Itomi³, M. Kobayashi¹, E. A. Drapiko⁴, and the LHD Experiment Group

¹National Institute for Fusion Science, Toki-shi, Gifu-ken 509-5292, Japan

²Graduate Univ. for Adv. Studies, Toki-shi, Gifu-ken 509-5292, Japan

³Hokkaido Univ., Sapporo, Hokkaido, Japan

⁴Kurchatov Inst., Moscow, Russia

Imaging Diagnostics Workshop

June 28, 2013

National Institute for Fusion Science

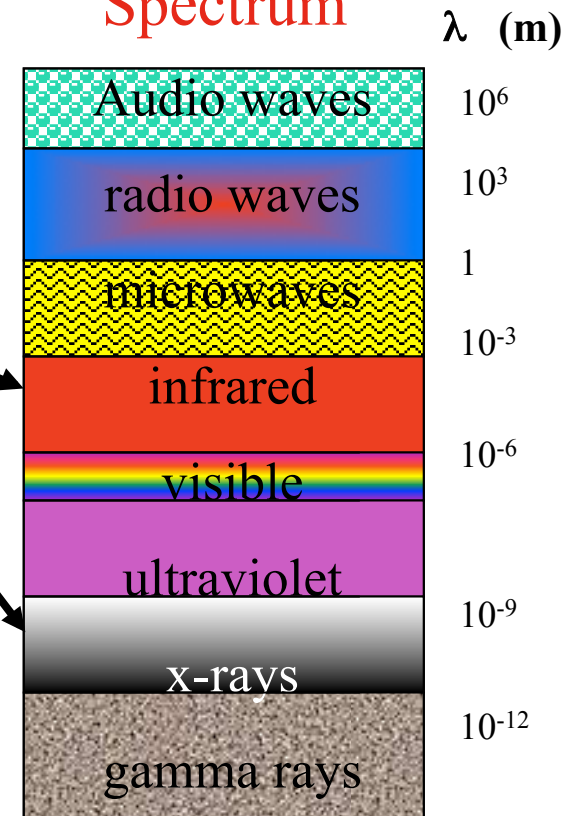


Outline

- IRVB concept
- IRVBs on LHD
- Calculation of geometry matrices
- Synthetic instruments vs tomography
- Detachment using magnetic island
- Conclusions

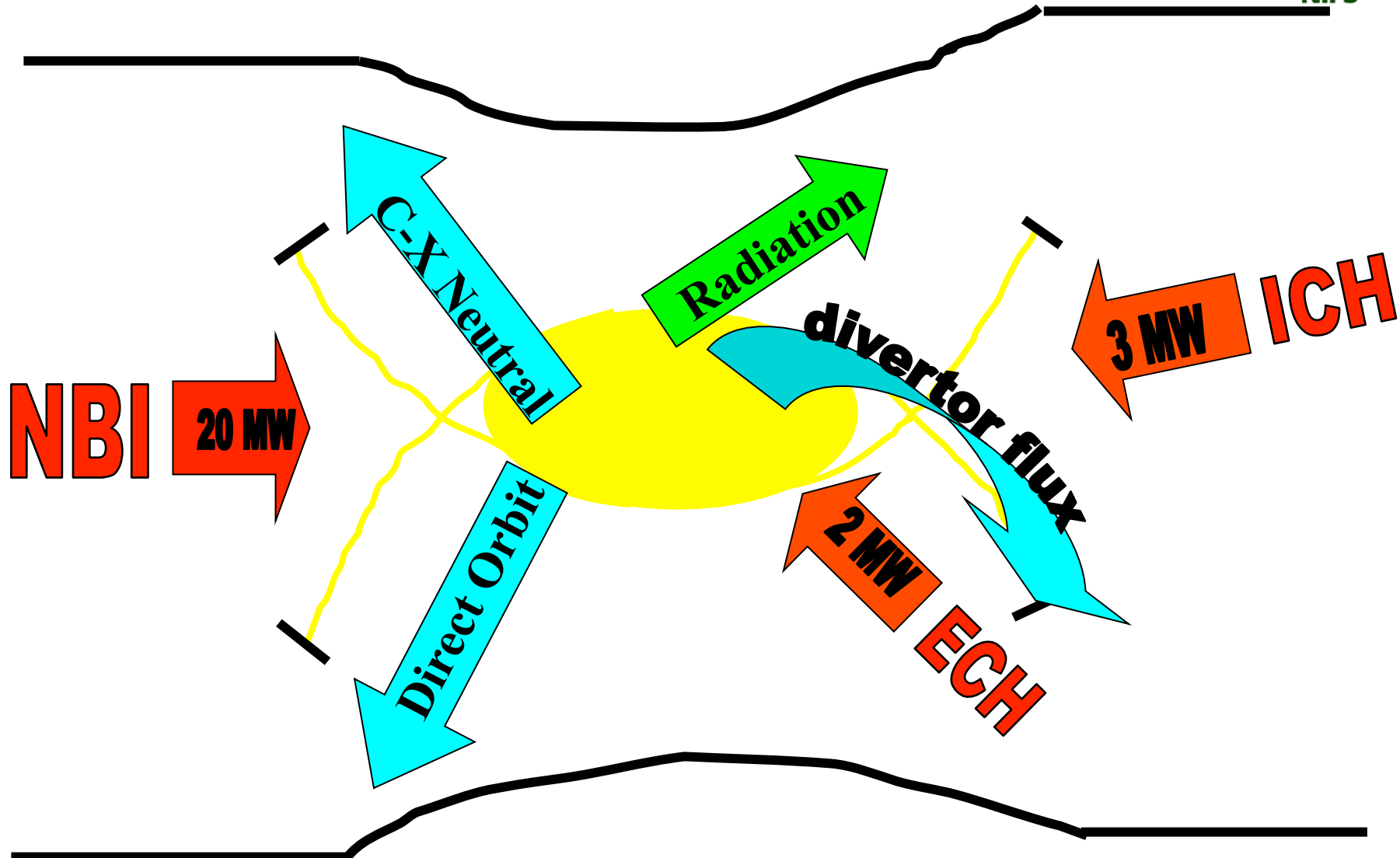
- Measures total radiation (and neutrals) from plasma
- From IR to soft x-rays
- Estimate radiative power loss for power balance
- Study role of impurities

Electromagnetic Spectrum



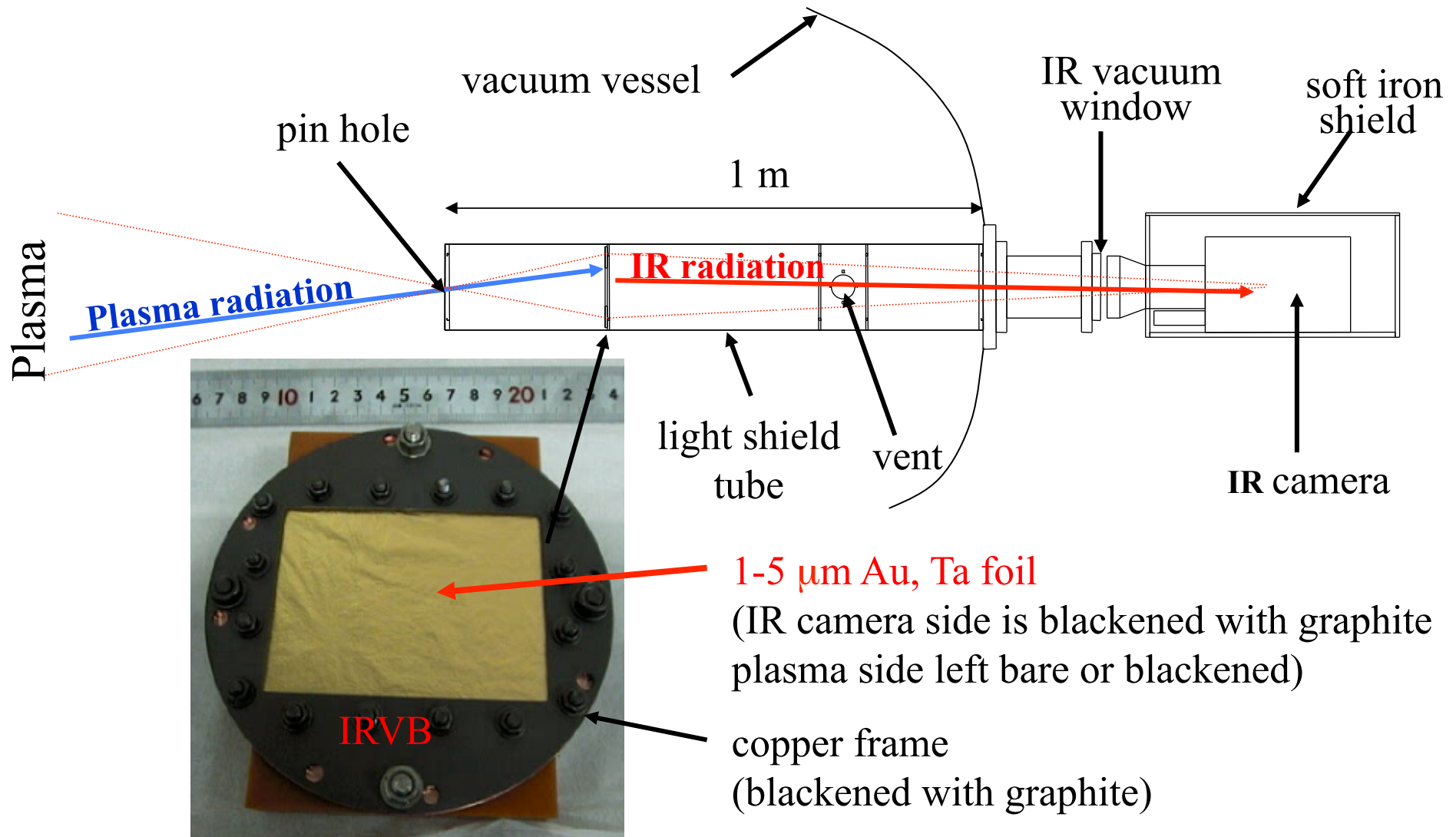


Power Balance (LHD)





IR imaging Video Bolometer (IRVB)





IRVB - Concept



Solve foil 2D heat diffusion equation for P_{rad}

$$-\Omega_{rad} + \Omega_{bb} + \frac{1}{K} \frac{\partial T}{\partial t} = \frac{\partial^2 T}{\partial x^2} + \frac{\partial^2 T}{\partial y^2}$$

2-D Laplacian

foil thermal diffusivity

$$\Omega_{bb} = \frac{\epsilon \sigma_{S-B} (T^4 - T_0^4)}{kt_f} \quad \epsilon \cong 1$$

black body cooling term

$$\Omega_{rad} = \frac{P_{rad}}{kt_f l^2}$$

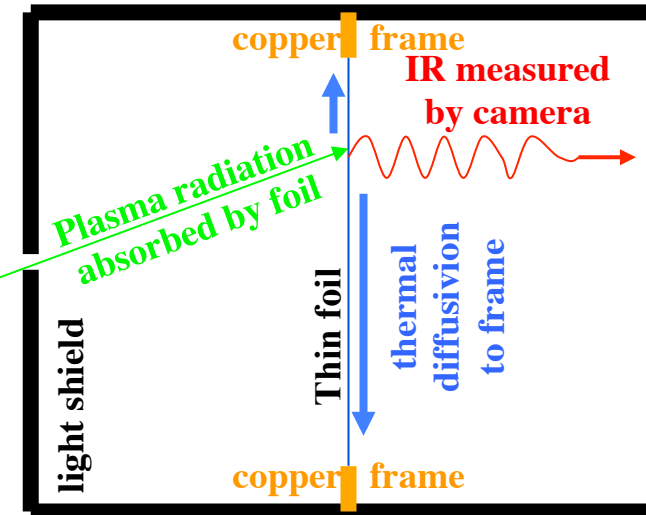
foil thermal conductivity

foil thickness

bolometer pixel area

plasma radiated power is determined by numerically solving heat diffusion equation using a Crank-Nicholson scheme

IRVB pinhole camera



IR Imaging video Bolometer (calibration technique)

The two-dimensional heat diffusion equation

Detected radiation
Power density from
solving heat
diffusion equation

$$S_{rad} = S_{bb} - C_s \frac{\partial T}{\partial t} - kt_f \left[\frac{\partial^2 T}{\partial x^2} + \frac{\partial^2 T}{\partial y^2} \right]$$

temperature on the foil

Black body radiation from the foil

foil surface thermal capacity

Foil thermal conductivity

Foil thickness

Parameters to be determined locally on the foil through calibration experiments

Blackbody thermal emissivity

$$S_{bb} = \epsilon \sigma_{S-B} (T^4 - T_0^4)$$

$$S_{rad} = \frac{P_{rad}}{l^2}$$

the incident radiation power to the foil

Bolometer pixel area

LHD: B.J.Peterson, et.al., Rev. Sci. Instrum. **74** (2003)2040

JT-60U: H.Parchamy, B.J.Peterson, et.al., Rev. Sci. Instrum. **77** (2006)515

LHD: E. A. Drapiko, et.al., Rev. Sci. Instrum. **81** (2010) 10E128.



4 IRVBs operating on LHD

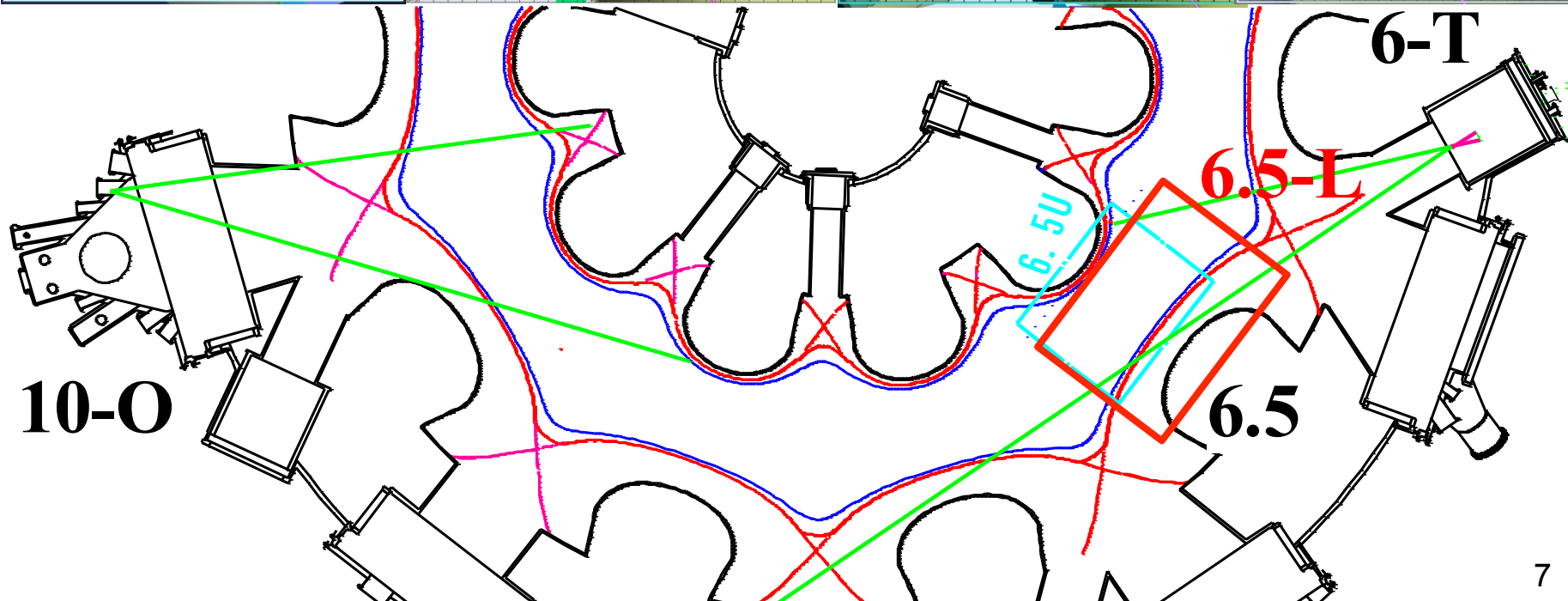
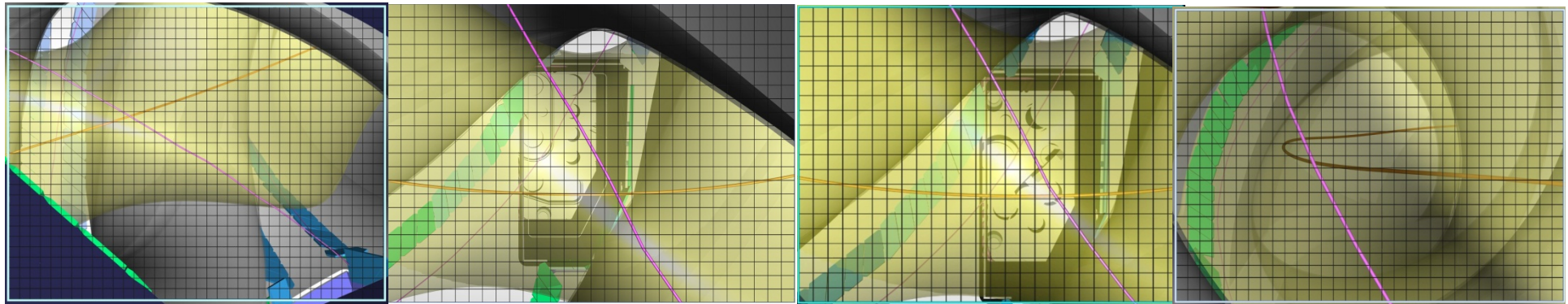
Total 2528 channels

Port 10-O 24x32 ch
(SC500 -> SC7600)

Port 6.5-L 20x28 ch
(Omega -> SC655)

Port 6.5-U 18x24 ch
(SC655)

Port 6-T 24x32 ch
(SC4000)





Geometry matrix calculation for synthetic diagnostic for LHD IRVB



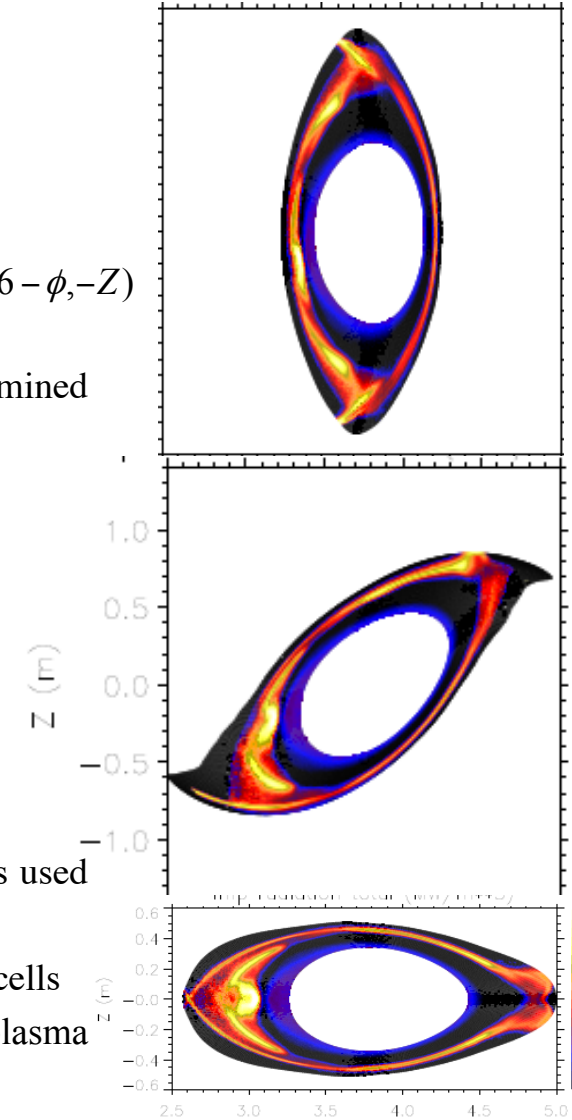
- Plasma is divided into volumes using R, z, ϕ
- $\Delta R = 5 \text{ cm}, \Delta z = 5 \text{ cm}, \Delta\phi = 1 \text{ degree}$
- $2.5 \text{ m} < R < 5.0 \text{ m}$ (50 divisions)
- $-1.3 \text{ m} < z < 1.3 \text{ m}$ (52 divisions)
- $\phi = 0 - 18 \text{ degrees}$ (18 divisions) assume helical symmetry $S(R, \phi, Z) = S(R, 36 - \phi, -Z)$
- total 46,800 cells
- Intersection of plasma volumes and bolometer chord volumes, V_{ij} , is determined using subvoxels $< 1 \text{ cm}$
- Solid angle, Ω_{ij} for the center of each subvoxel is calculated

$$\Omega_{i,j} = A_{\text{det}} / d^2$$

- Write system of equations for detector power, P_i , and volume emissivity, S_j

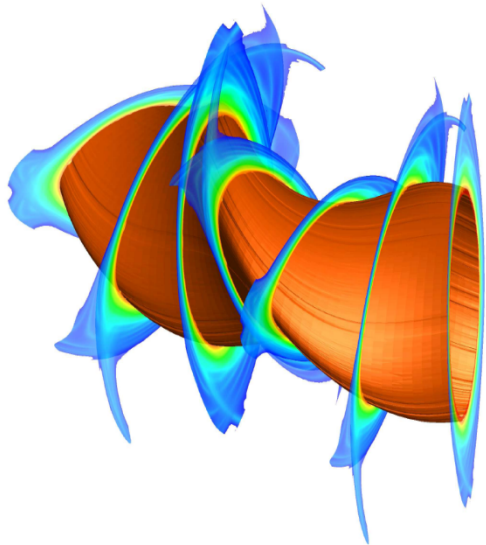
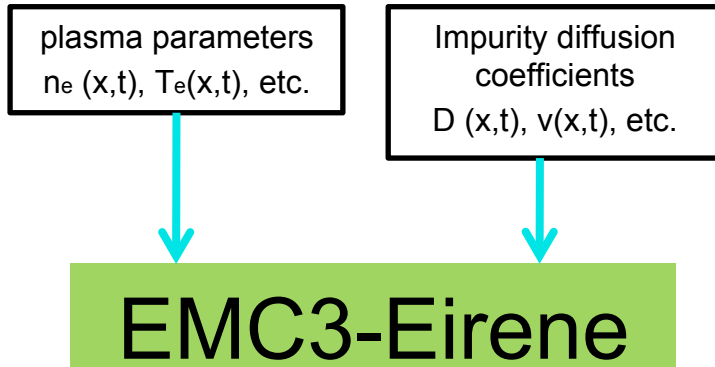
$$P_i = \sum_j \frac{\Omega_{ij}}{4\pi} V_{ij} S_j = \sum_j T_{ij} S_j$$

- Then geometry matrix, T_{ij} , is determined
- 3-D C radiation data from EMC3-EIRENE is resampled to $5 \text{ cm} \times 5 \text{ cm} \times 1^\circ$ is used as S_j to calculate P_i at detector
- Use code data to remove non-radiating voxels from edge (by factor 4) to 13,161 cells
- At each step location of subvoxels is checked to make sure it is within plasma subvolume region and does not intersect wall.
- avg 44 sightlines per voxel, maximum is 113
- All plasma voxels can be seen by at least one IRVB channel



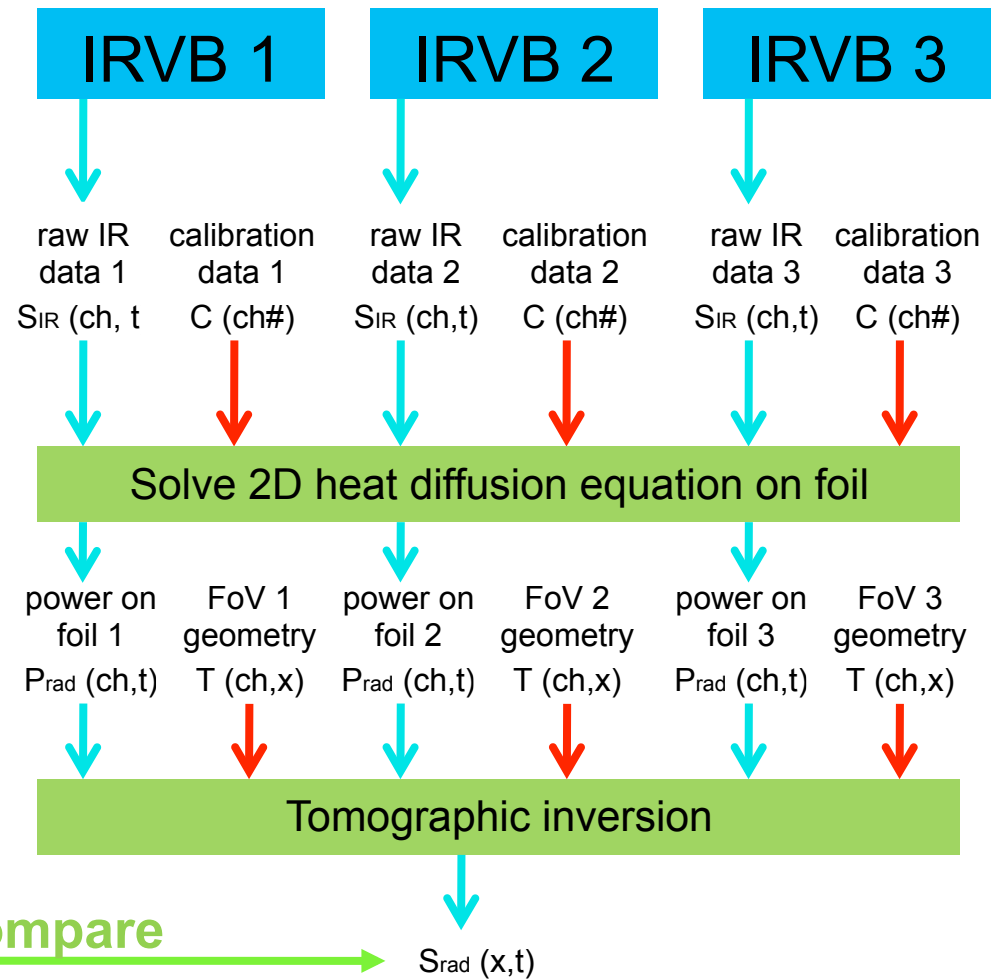
Tomography – applied to imaging bolometers

Impurity transport model



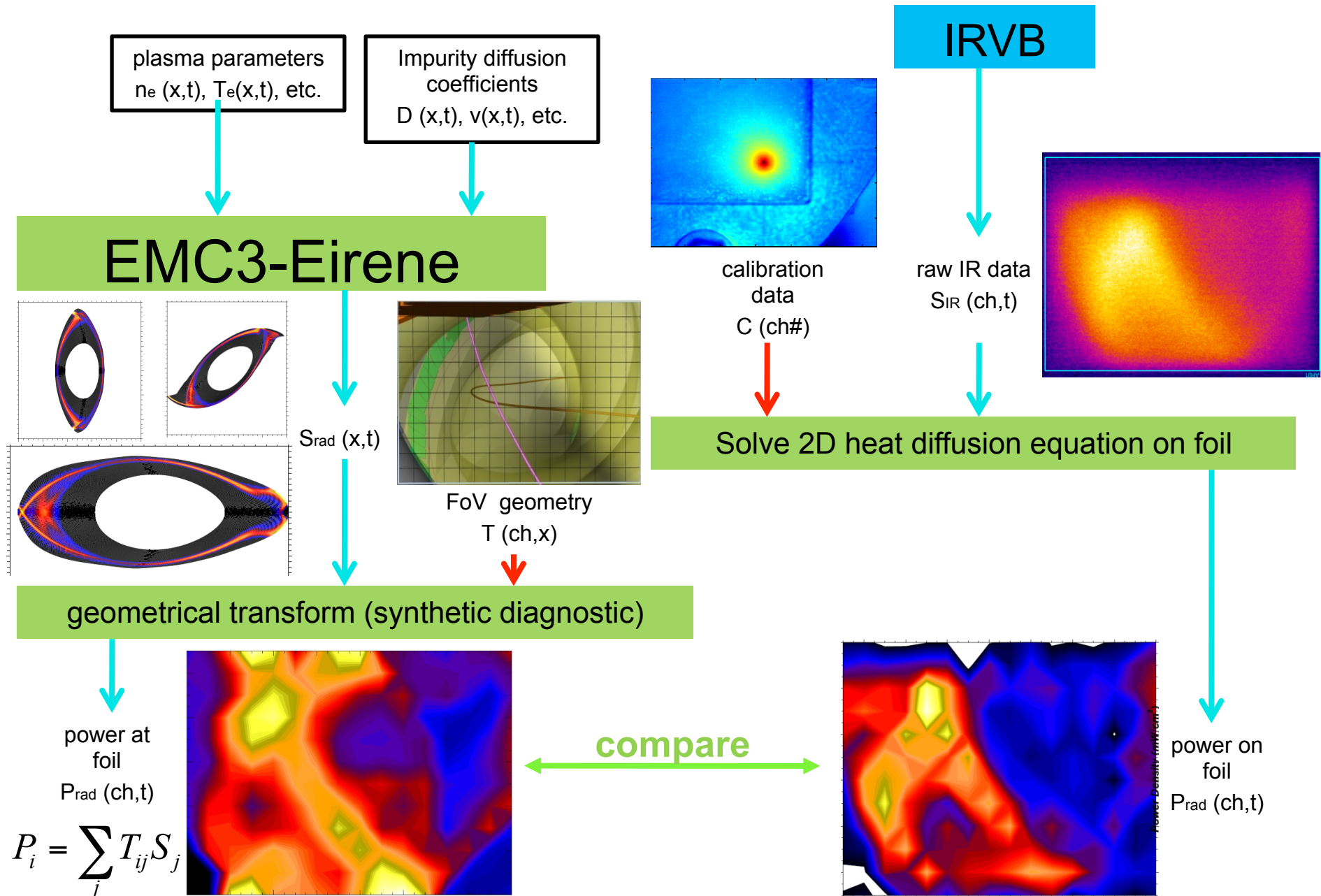
$S_{rad}(x,t)$

IRVB



See next presentation by R. Sano

Synthetic diagnostic – applied to imaging bolometer



Calculation of matrices and synthetic image from EMC3-EIRENE model

Step :1

Emissivity Matrix

Regularize and resample EMC3-EIRENE data to 5 cm X 5 cm X 1° grid for every field period

Stack the re-sampled data from all the field periods to give S_j matrix

Step :2

Geometry Matrix

Plasma is divided into volumes using R, z, ϕ
 $\Delta R = 5 \text{ cm}, \Delta z = 5 \text{ cm}, \Delta \phi = 1^\circ$
 where
 $2.5 \text{ m} < R < 5.0 \text{ m}$ (50 divisions)
 $-1.3 \text{ m} < z < 1.3 \text{ m}$ (52 divisions) & $\phi = 0 - 180^\circ$
 (total 468,000 cells)

Intersection of plasma volumes and bolometer chord volumes, V_{ij} is determined using subvoxels $< 1 \text{ cm}$

Solid angle, Ω_{ij} for the center of each sub-voxel is calculated $\Omega_{i,j} = A_{\text{det}} / d^2$

Geometry matrix, T_{ij} is determined as $T_{ij} = \frac{\Omega_{ij}}{4\pi} V_{ij}$

Step :3

Detector Power

Detector power, P_i can be determined by multiplying geometry matrix and emissivity matrix

$$P_i = \sum_j \frac{\Omega_{ij}}{4\pi} V_{ij} S_j = \sum_j T_{ij} S_j$$

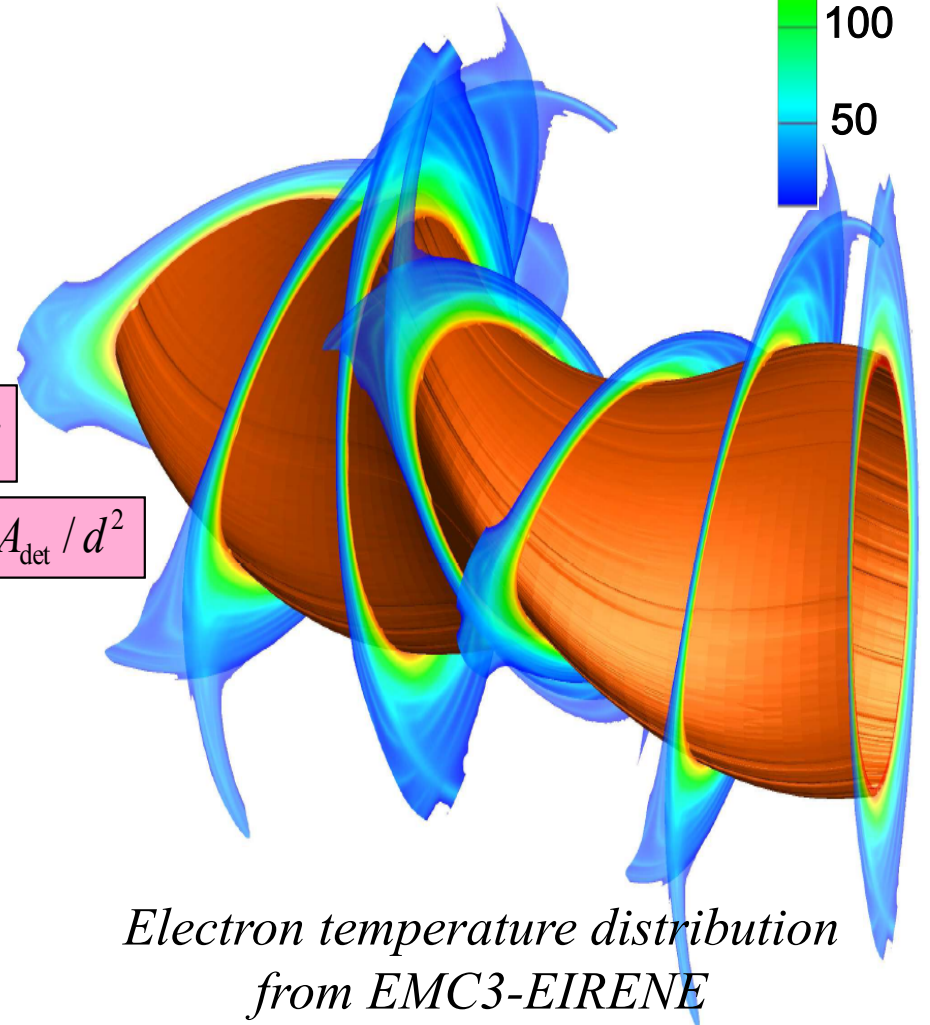
Te (eV)

200

150

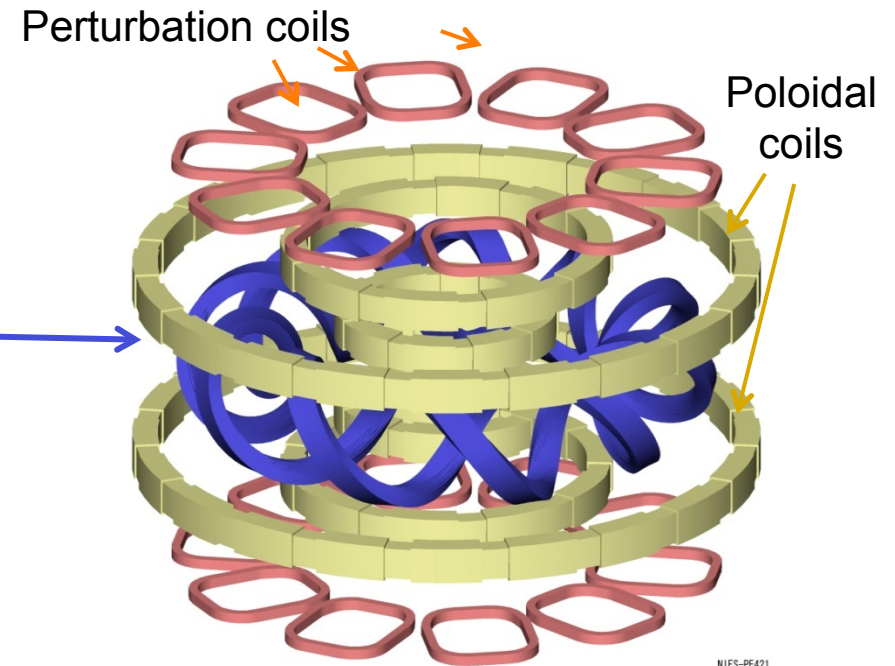
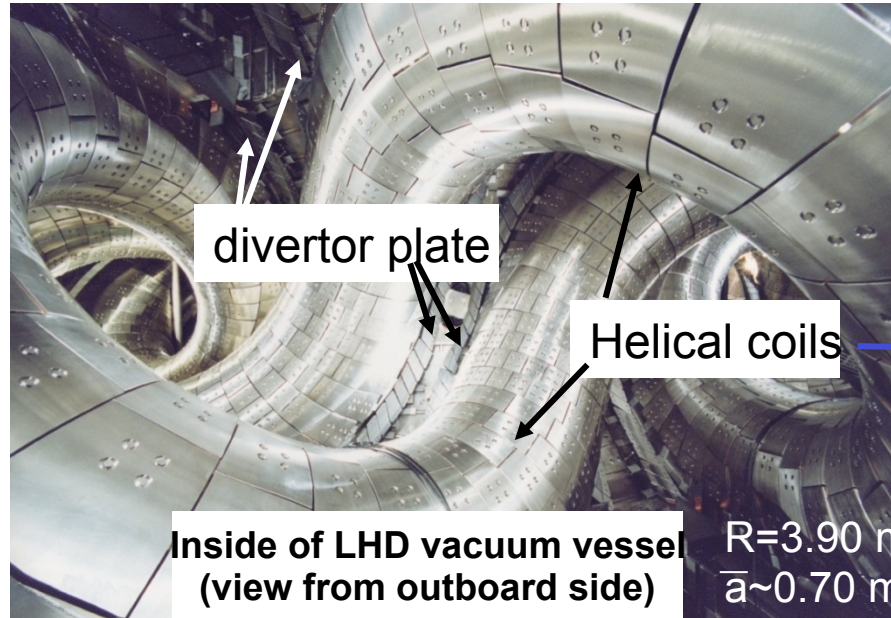
100

50

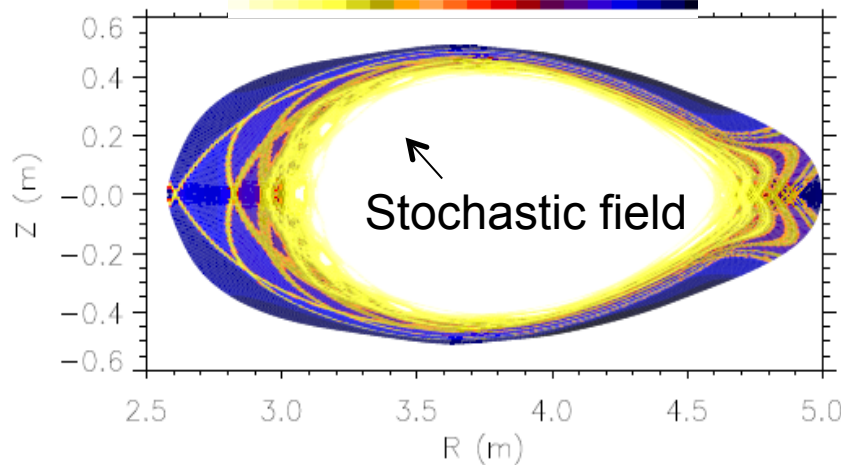
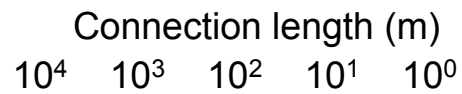


Electron temperature distribution from EMC3-EIRENE

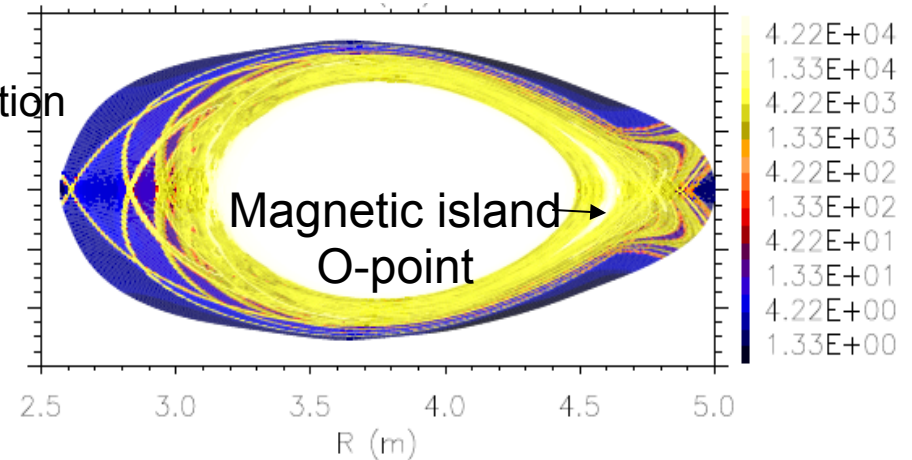
Edge stochastic magnetic field and modification by $n/m=1/1$ resonant perturbation



NIFS-PE421

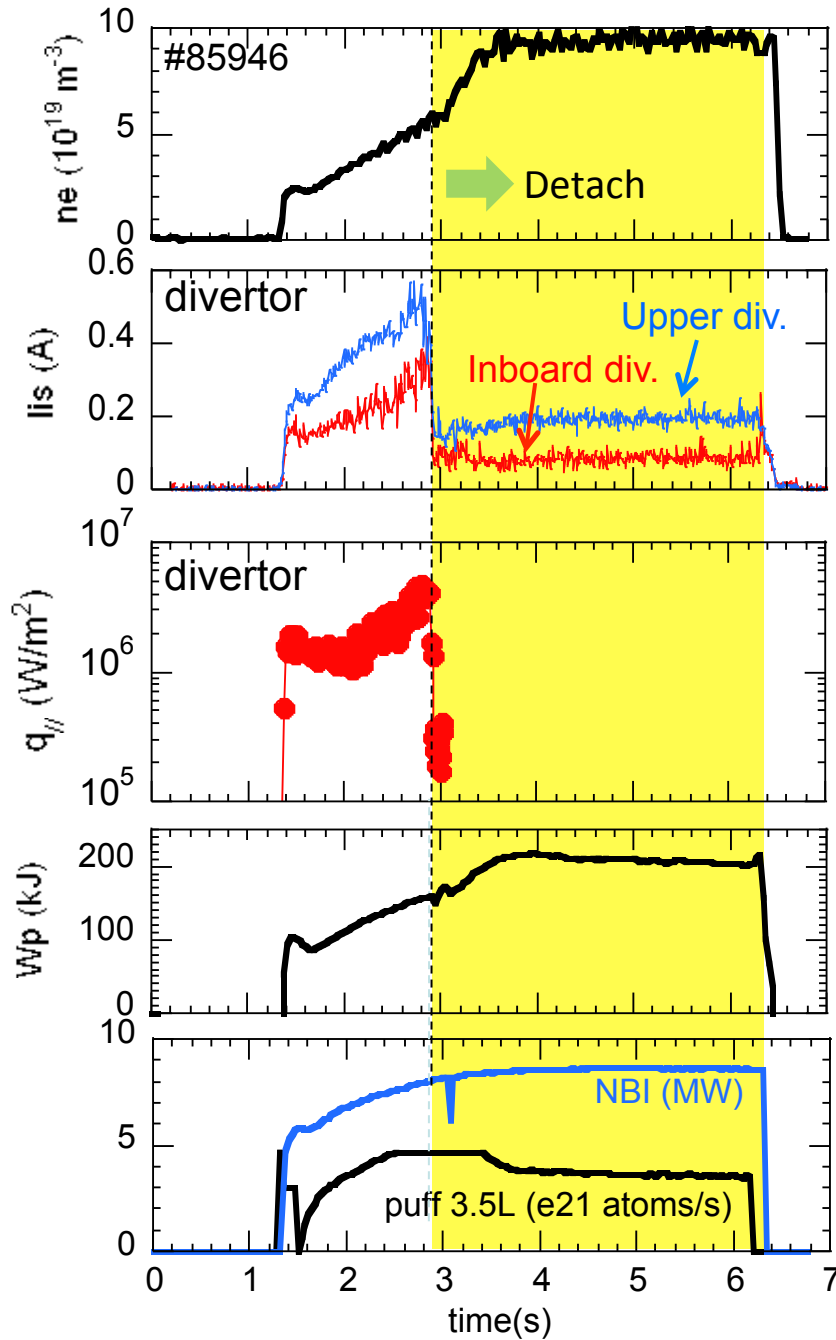


$n/m=1/1$ perturbation

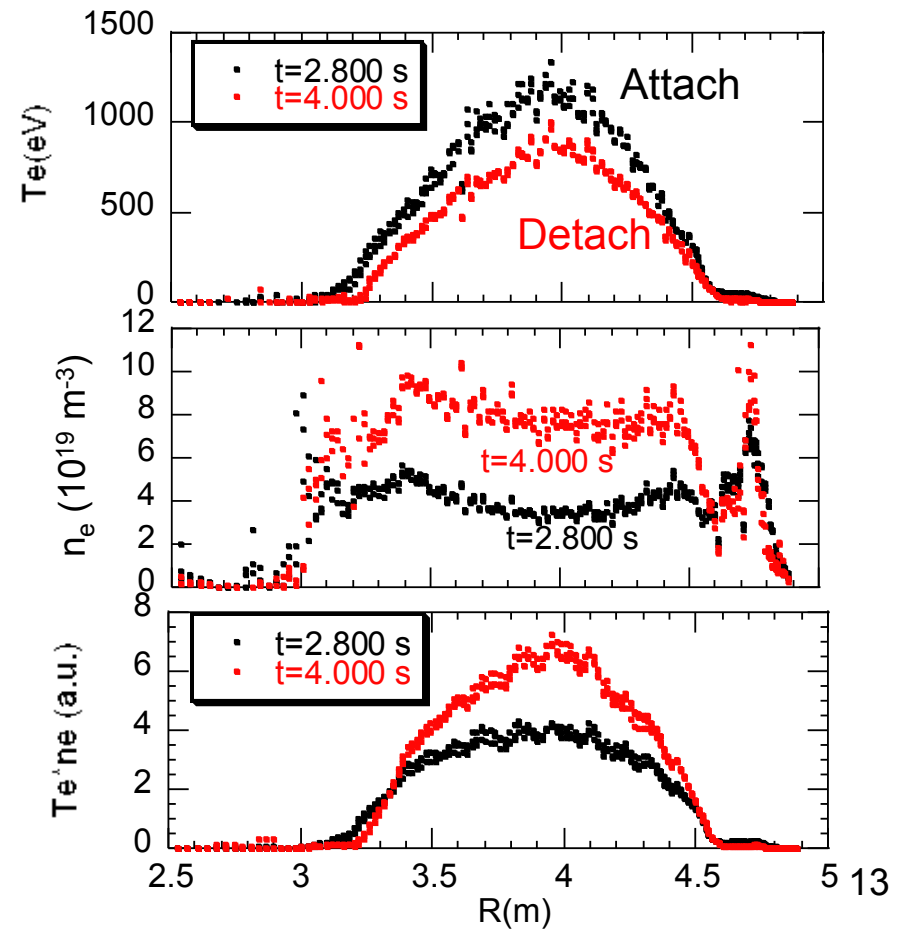


Large flexibility in changing field structure of LHD edge region:
1/1 Island size, radial/toroidal location, stochastic boundary thickness

Sustained detachment with application of n/m=1/1 island



1/3 reduction of divertor particle flux
 1/10 reduction of divertor energy flux
 The discharge was terminated by stop of NBI heating.
 No confinement degradation, even slight improve.

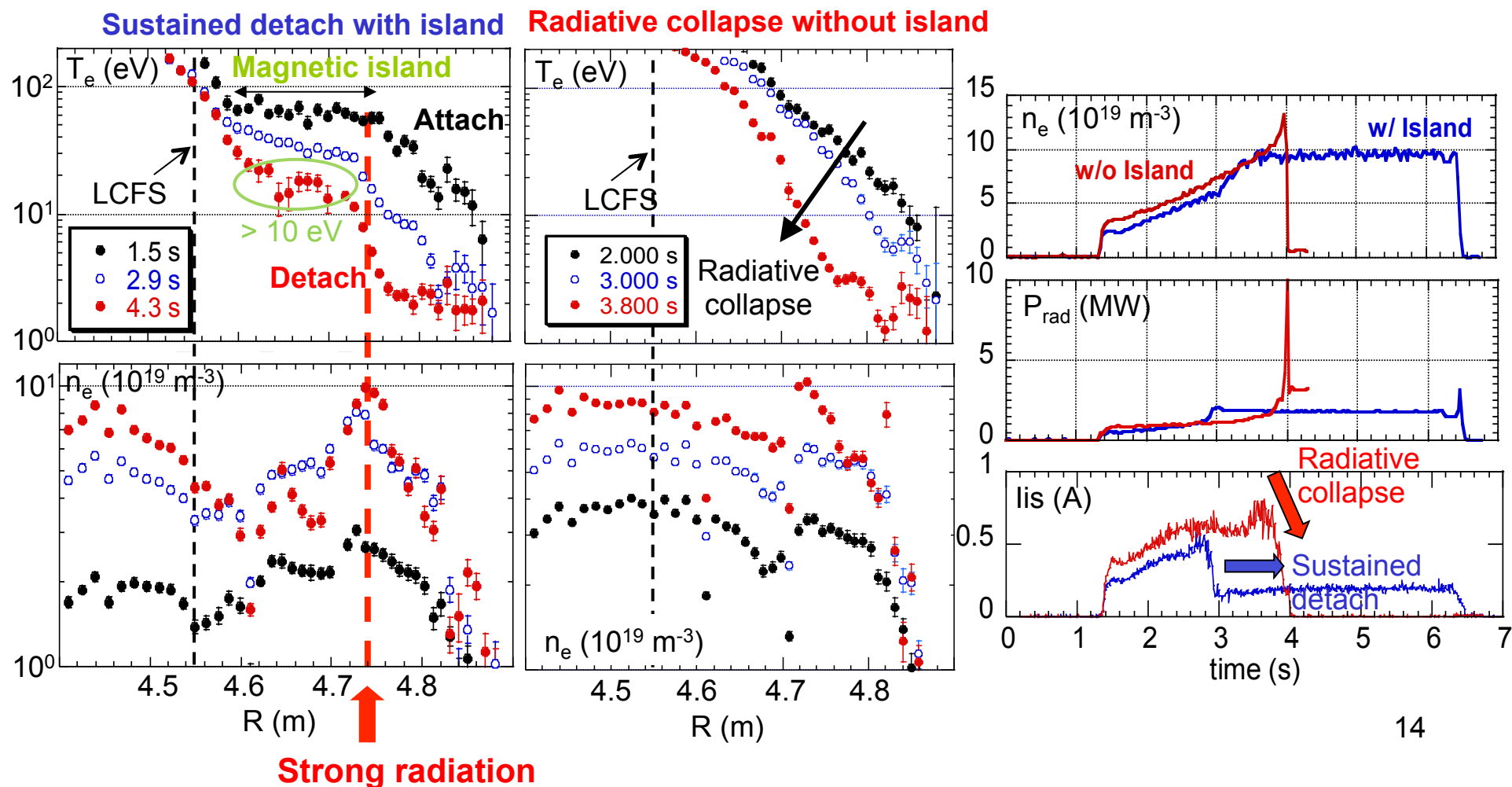


The island structure seems to stop radiation region penetrate inward

Inside island parallel transport dominant

- kept more than 10 eV > carbon radiation peak T_e
- Stop radiation region penetrate inward
- few eV & 10^{20} m^{-3} plasma (strong radiation) outside LCFS
- Indicates strong radiation around separatrix

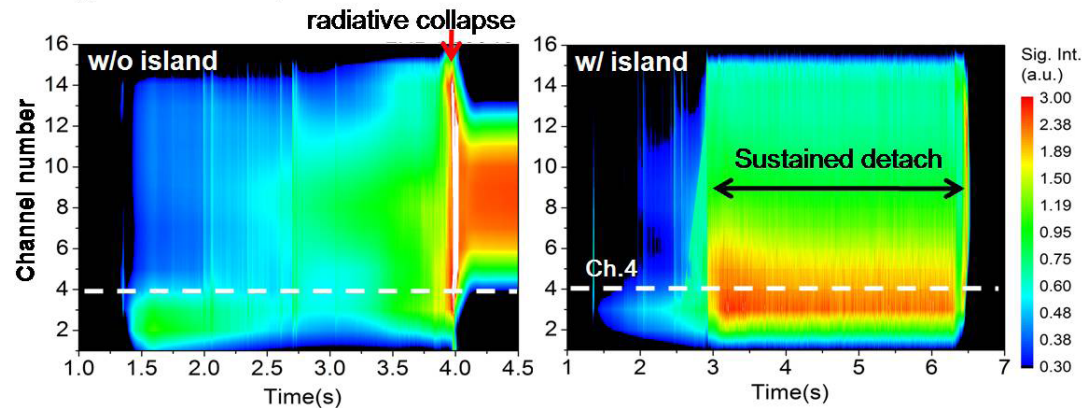
Density ramp up leads to radiative collapse without n/m=1/1 island.



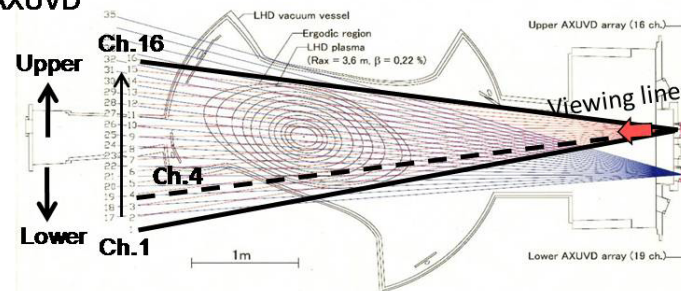


Detached plasma with magnetic island in LHD

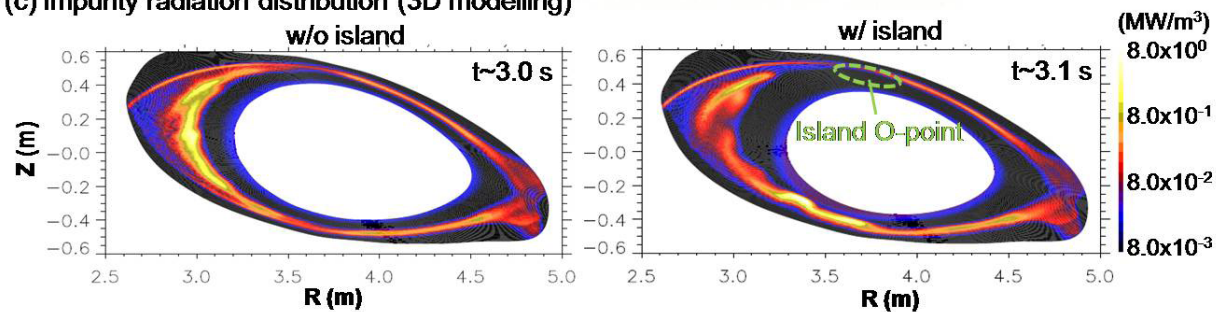
(a) Line integrated radiation profiles (AXUVD)



(b) Viewing lines of AXUVD



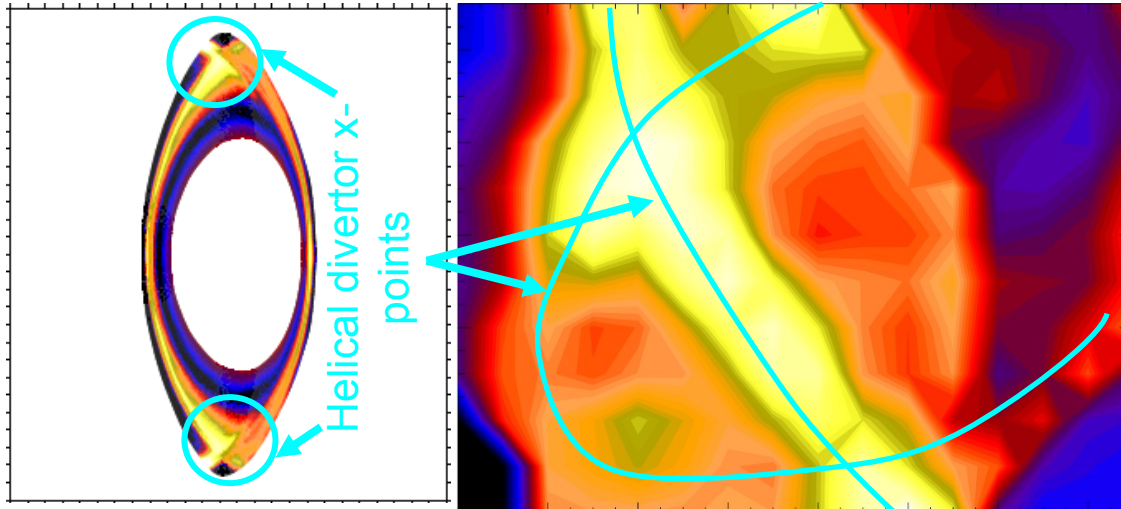
(c) Impurity radiation distribution (3D modelling)



Radiation Localization at HD X-points with Magnetic Island

C radiation data from EMC3-EIRENE

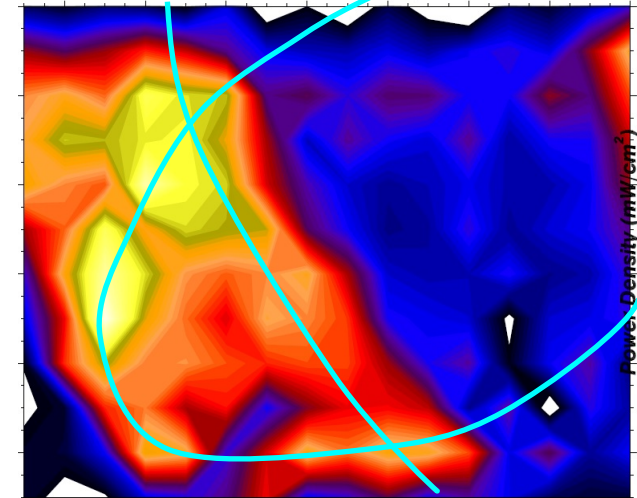
no island, $n_{LCFS} = 4 \times 10^{19}$, attached



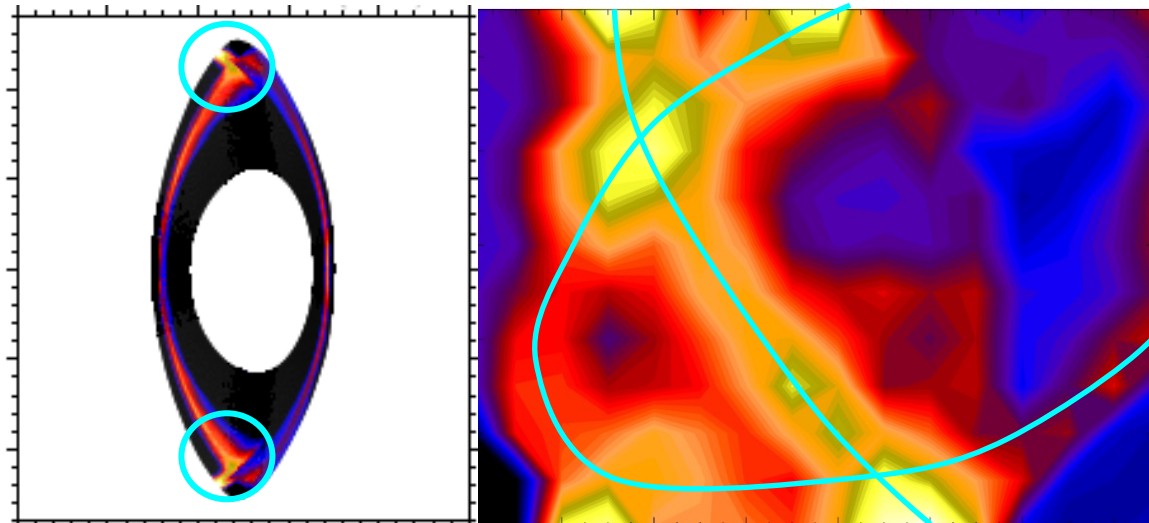
Imaging bolometer data

Shot 97365, $t=4.5$ s

no island, $n_e = 5 \times 10^{19}$, attached

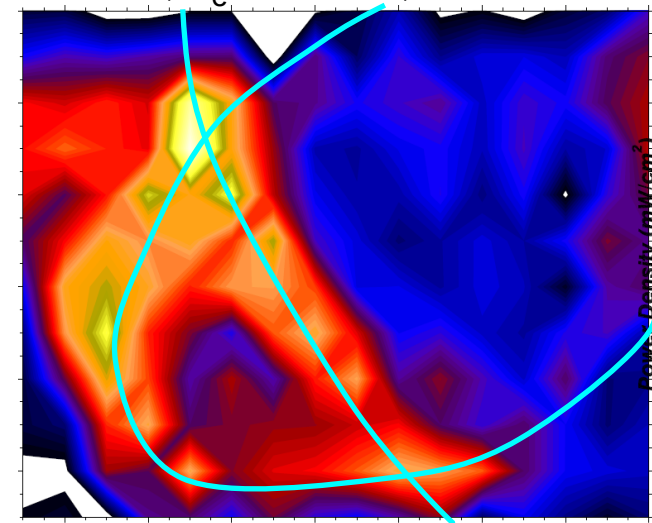


with island, $n_{LCFS} = 4 \times 10^{19}$, attached



Shot 97327, $t=4.5$ s

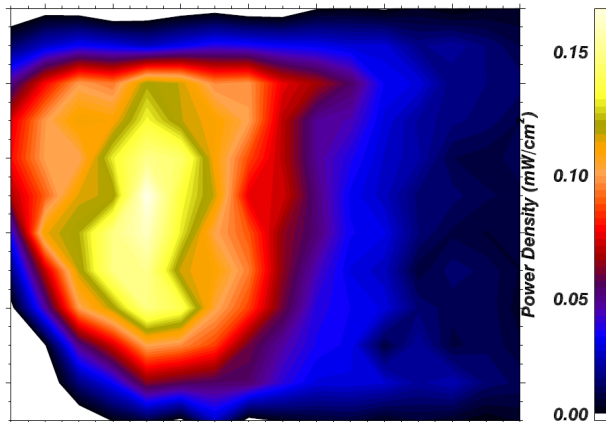
with island, $n_e = 5 \times 10^{19}$, attached



Radiation becomes more well defined in helical divertor with increasing density and the addition of magnetic island

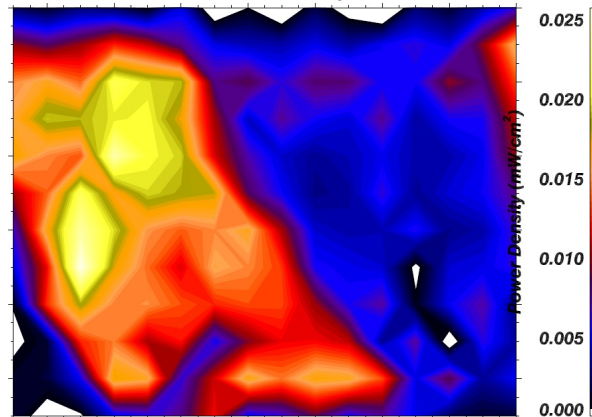
Shot 97353, $t=5.3$ s

no island, $n_e = 1.5 \times 10^{19}$
attached



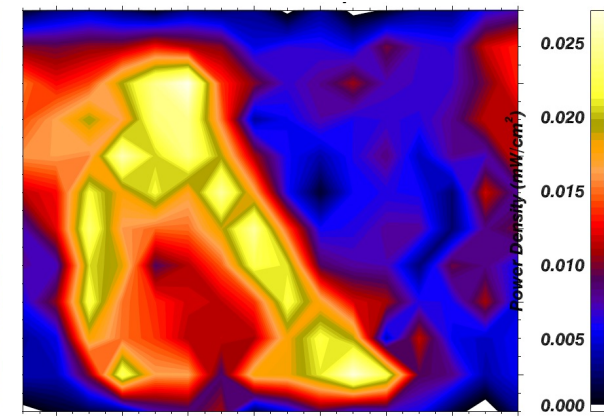
Shot 97365, $t=4.5$ s

no island, $n_e = 5 \times 10^{19}$
attached



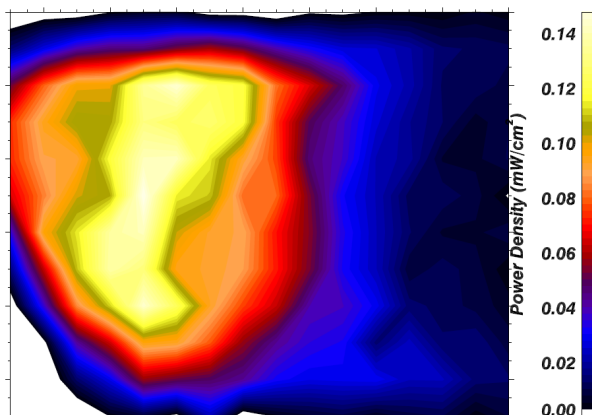
Shot 97365, $t=6.0$ s

no island, $n_e = 7 \times 10^{19}$ attached



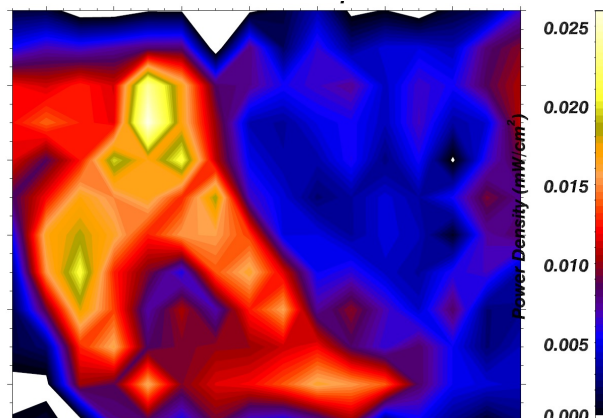
Shot 97354, $t=5.3$ s

with island, $n_e = 1.5 \times 10^{19}$
attached



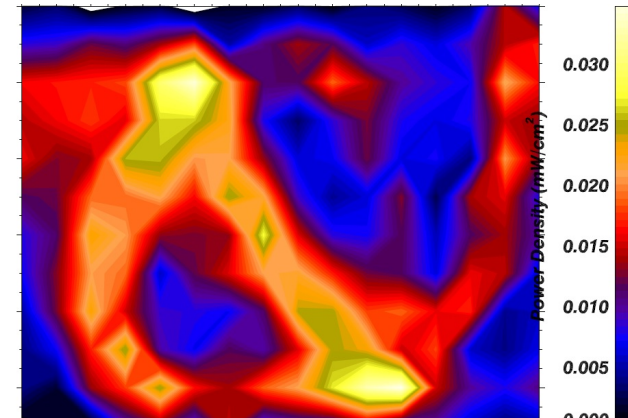
Shot 97327, $t=4.5$ s

with island, $n_e = 5 \times 10^{19}$
attached



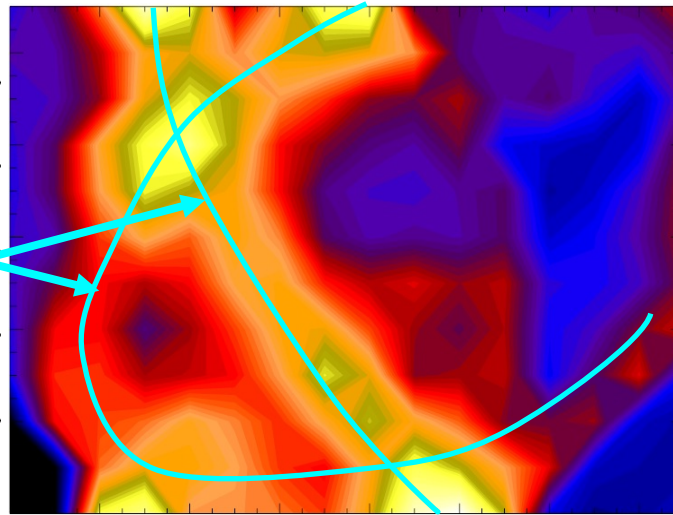
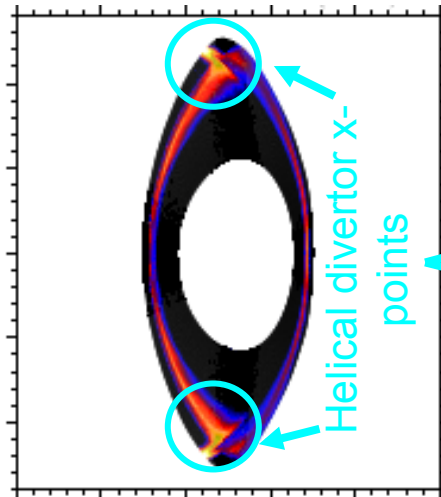
Shot 97327, $t=6.0$ s

with island, $n_e = 6 \times 10^{19}$
detached

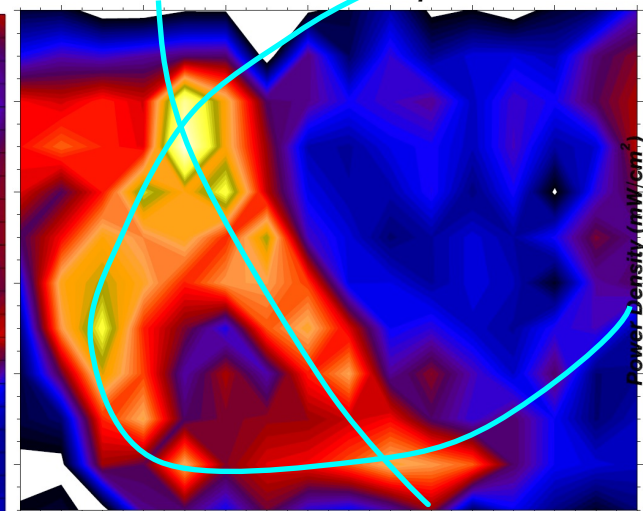


Increase in MI X-point Radiation with Detachment

C radiation data from EMC3-EIRENE
with island, $n_{\text{LCFS}} = 4 \times 10^{19}$, attached

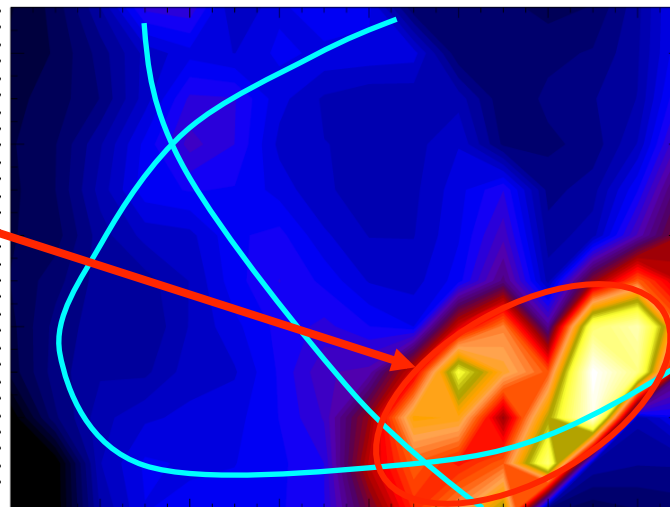
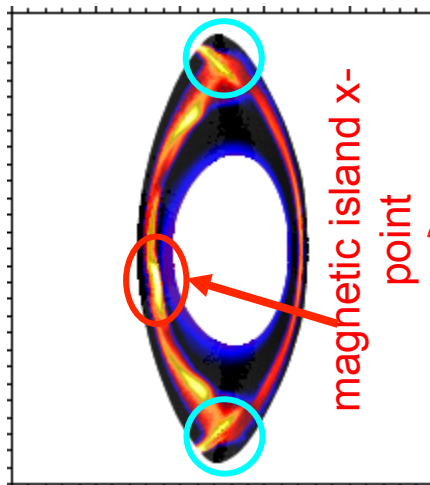


Imaging bolometer data
with island, $n_e = 5 \times 10^{19}$, attached

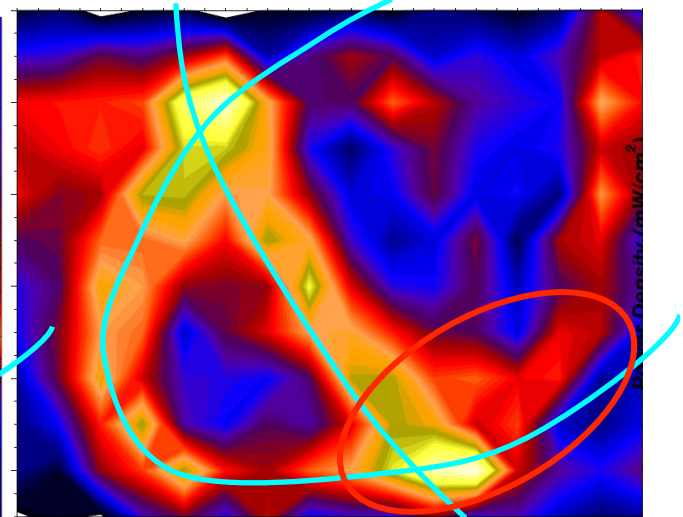


MI x-point radiation increases with detachment as predicted but overestimated by code

with island, $n_{\text{LCFS}} = 5.5 \times 10^{19}$, detached



with island, $n_e = 6 \times 10^{19}$, detached

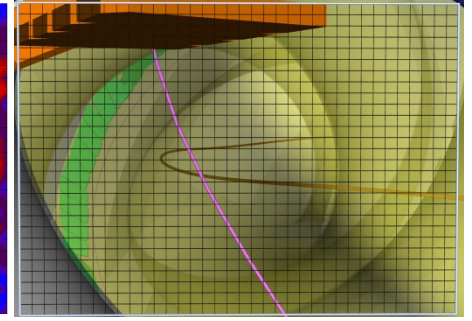
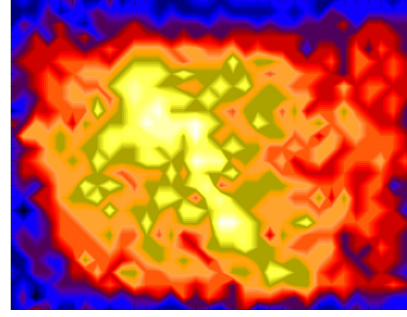
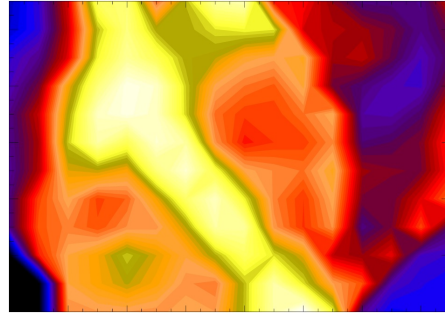
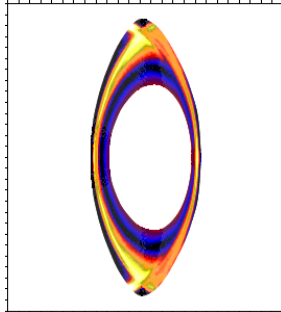




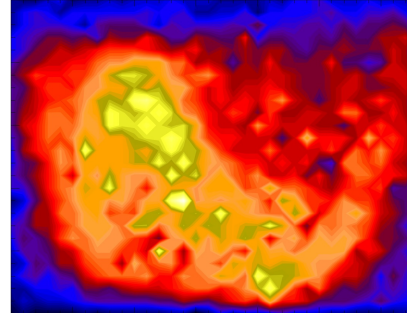
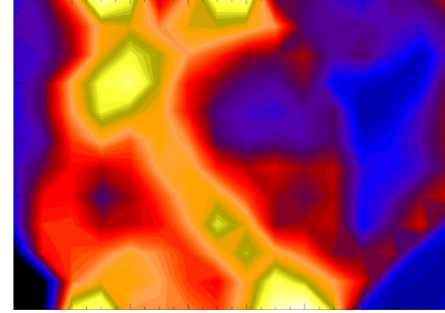
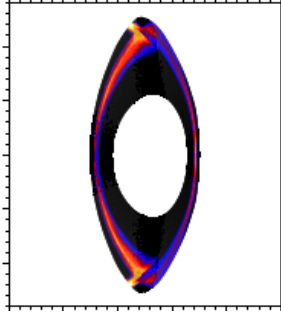
Detached plasma with magnetic island in LHD viewed from 6-T

Model – pol. xsection Model – synth. instrum. Experiment - IRVB

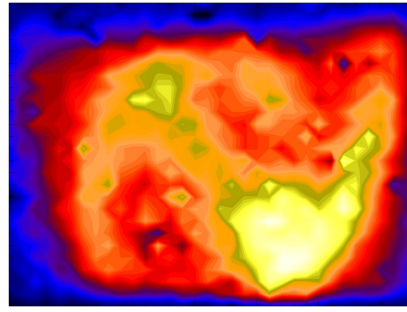
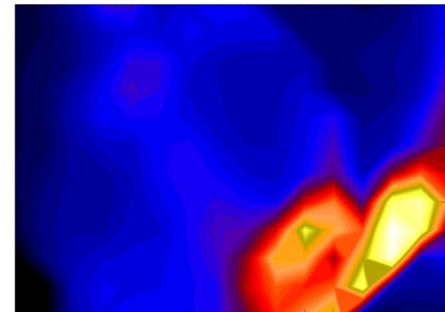
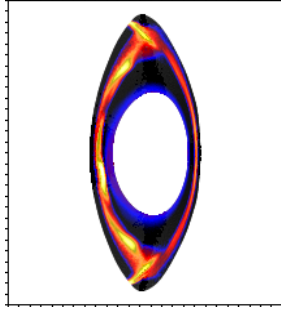
without MI
attached



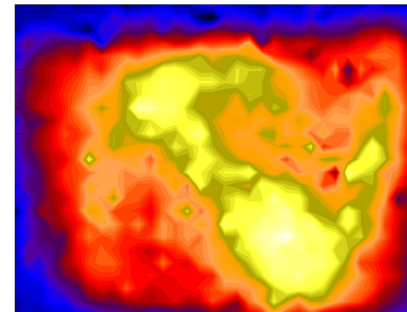
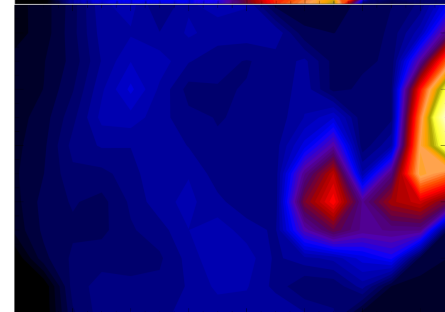
with MI at 6-O
attached



with MI at 6-O
detached



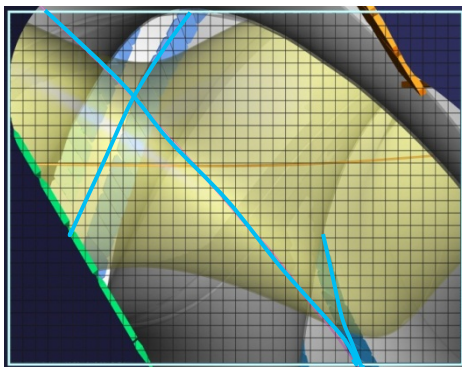
with MI at 7-O
detached



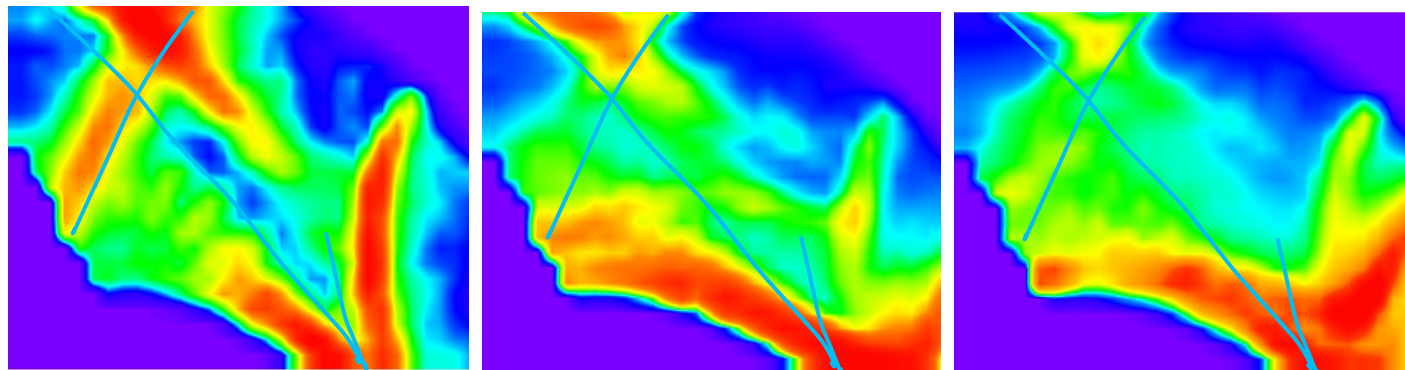


Detached plasma with magnetic island from LHD port 10-O

CAD view from
Port 10-O



Synthetic Images from EMC3-EIRENE data



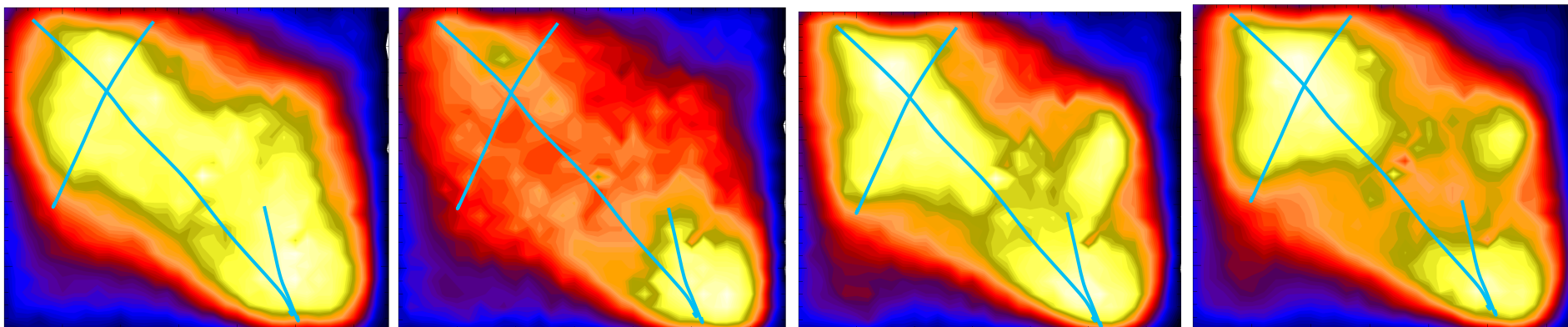
IRVB data

No MI attached

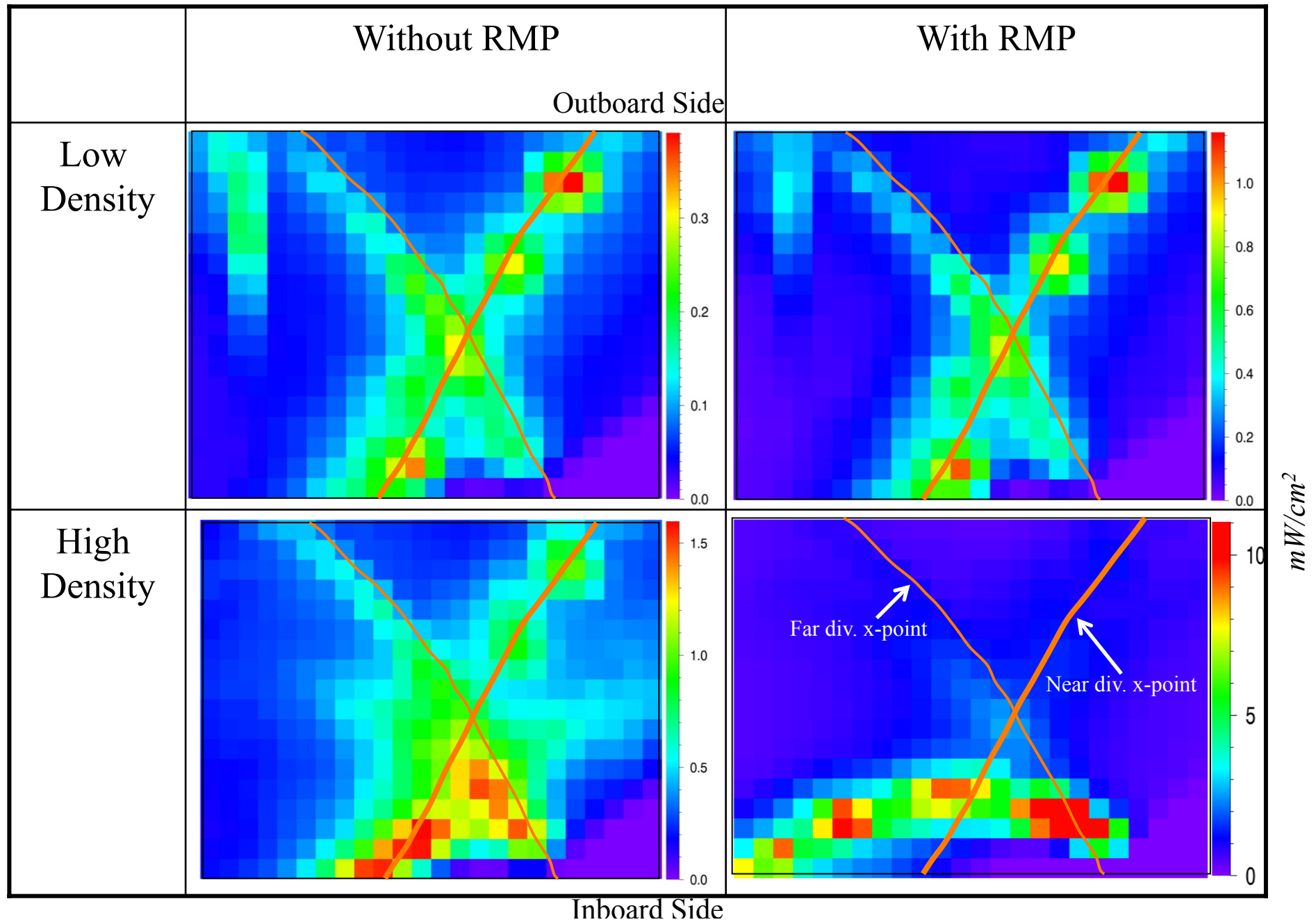
with MI at 6-O
attached

with MI at 6-O
detached

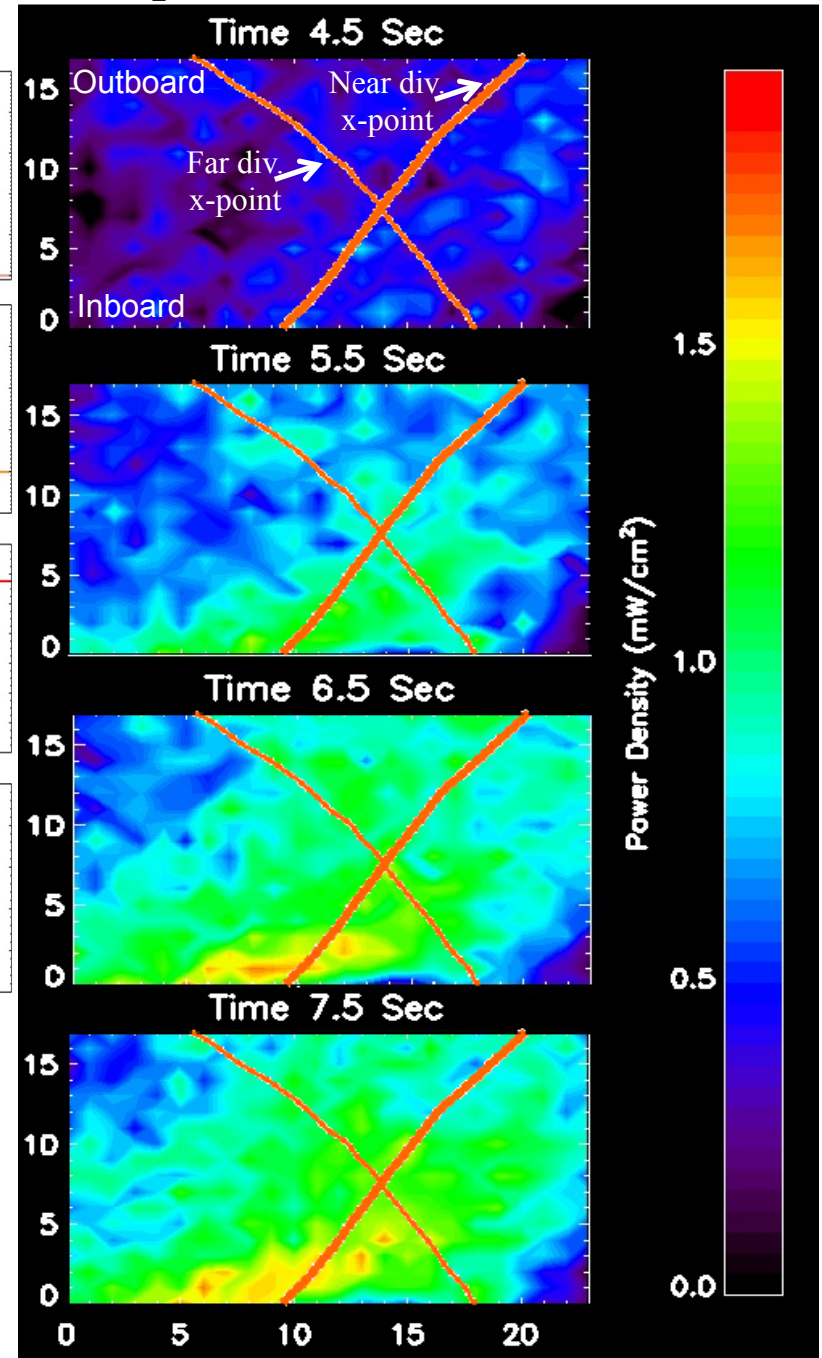
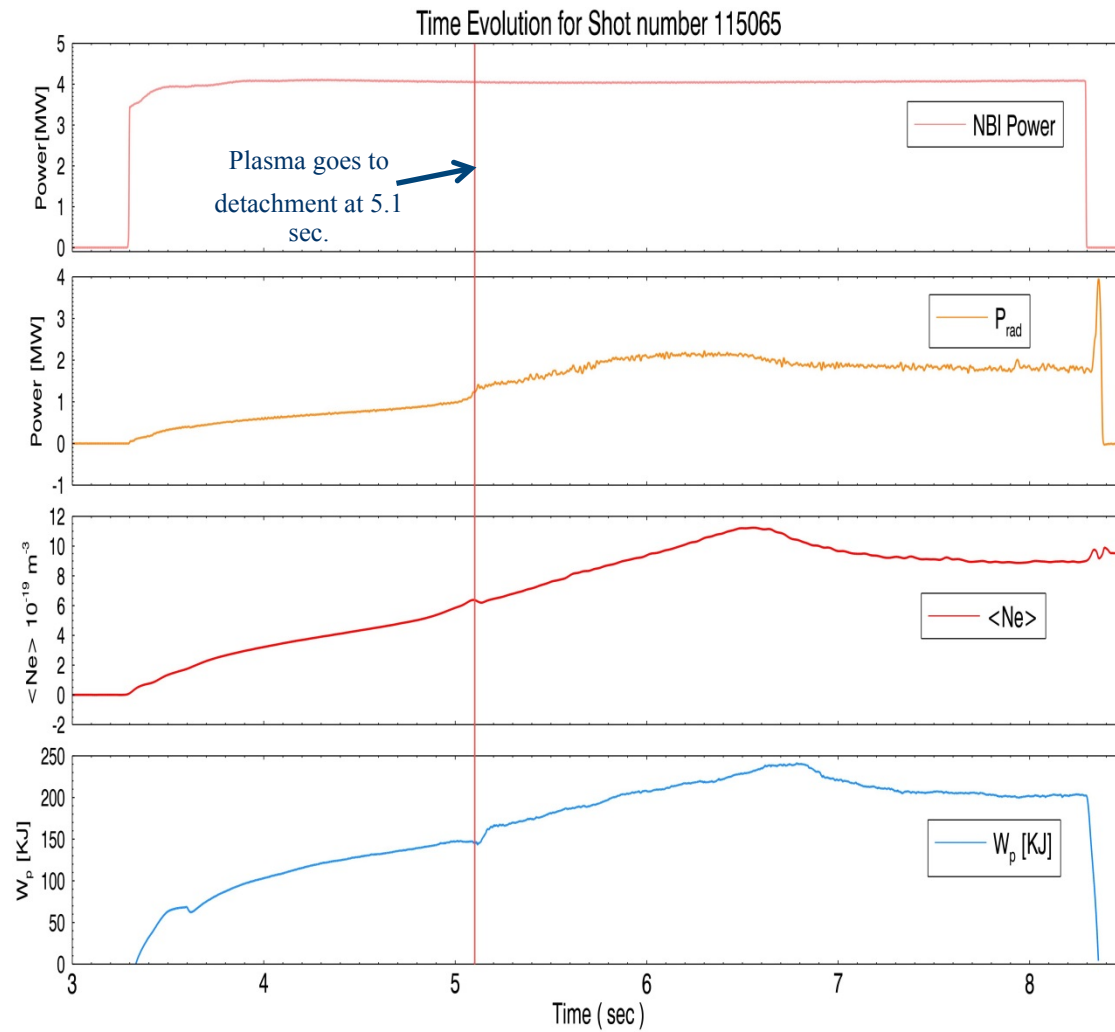
with MI at 7-O
detached



Model predicts radiation localization in island X-point during detachment



Experiment shows radiation localization near island X-points as detachment occurs



Experiment and Modeling – a comparison

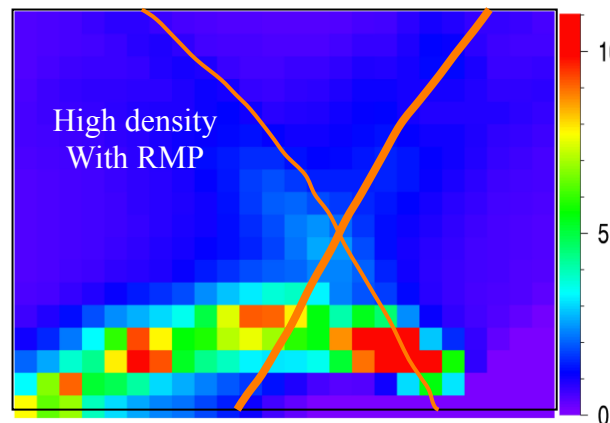
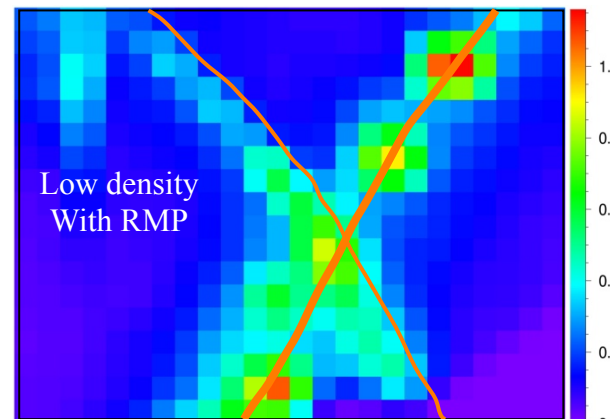
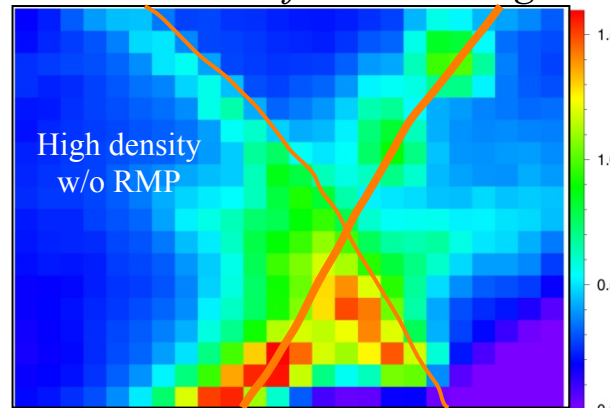
General observations

- Modeling – radiation along far and near divertor X-point trace
- Experiment – stronger radiation from near divertor X-point
- Power densities nearly match

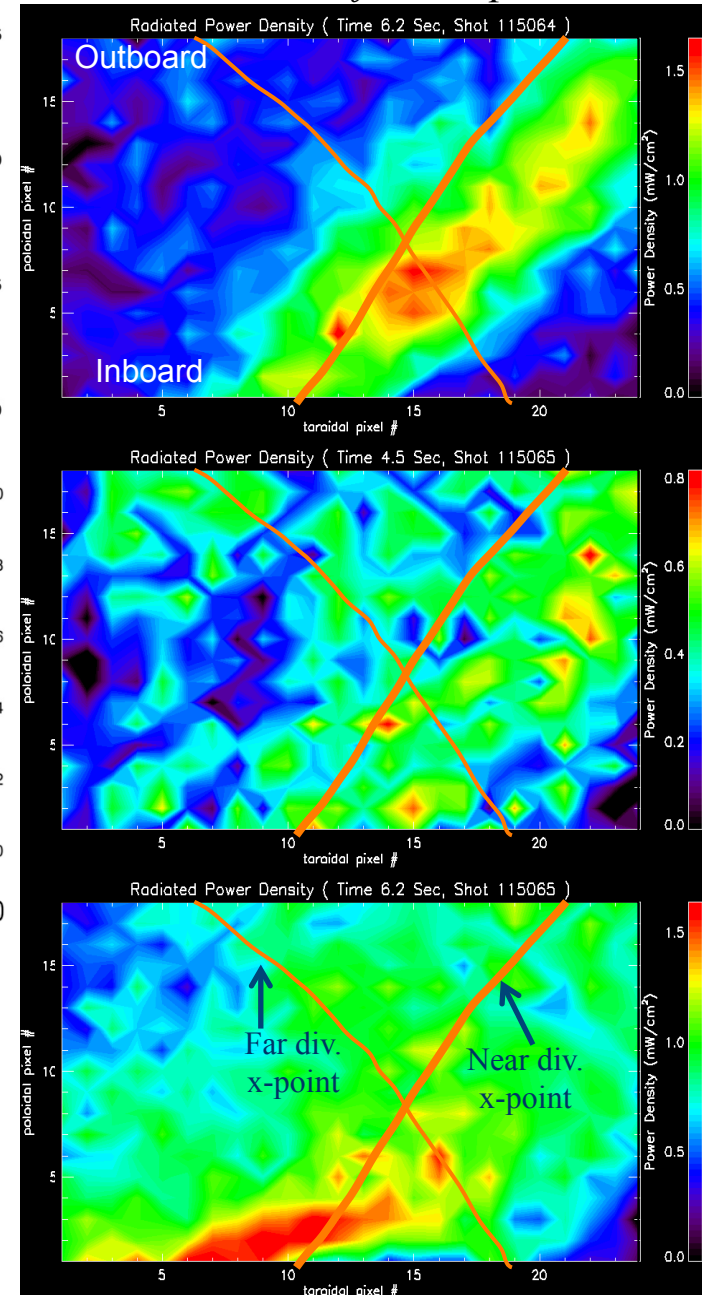
- Modeling – radiation along far and near divertor X-point trace
- Experiment – radiation from both near and far divertor X-points
- Power densities nearly match

- Modeling and experiments shows radiation localization near the island X-point towards inboard side
- Modeling - power densities 7 times higher than experiments
- The change in radiation pattern is similar both in modeling and experiments

Carbon radiation from modeling



Plasma radiation from Experiment





Conclusions and Future Research



- Last year's results
 - Three Imaging bolometers are installed on LHD
 - Ports 10-O, 6-T , 6.5-L and 6.5-U
 - 6-T and 10-O (24 x 32 channels each)
 - 6.5-U 18 x 24 ch
 - 6.5-L 20 x 28 (total 2528 ch)
 - laser calibration data is being analyzed (Itomi)
 - Study of detached plasma with and without island (Pandya, Drapiko, Peterson)
 - geometry matrices have been calculated for all IRVBs (Peterson, Sano)
- This year's plan
 - Operate IRVBs at 6-T (SC4000), 10-O (SC500), 6.5-L (Omega) to study:
 - Evolution of Magnetic island assisted detached plasmas (Pandya)
 - 3-D properties of asymmetric radiative collapse (Sano)
 - install periscope at 6.5-U (Pandya)
 - Optimize FOVs at 6-T and 10-O using geometry matrix program (Peterson, Sano)
 - Sample data (from code and measurements) and geometry matrices to Iwama, Teranishi et al. for development of 3D tomography software (Sano)
 - Finish analyzing calibration data and incorporate into analysis for absolute measurements (Itomi, Pandya, Sano)



Upgrade IRVBs on LHD

- Currently 4 IRVBs on LHD (2528 ch)
 - tangential (6-T) (24 x 32 ch) (SC4000)
 - semi-tangential (10-O) (24 x 32 ch) (SC500 -> SC7600)
 - top (6.5-U) (18 x 24 ch) (SC655, add periscope)
 - bottom (6.5-L) (20 x 28 ch) (omega -> SC655)
- increase number of channels in 2014
 - add radial (8-O) (24 x 32 ch) (SC655) (direct view of closed divertor)
 - Increase lower (6.5-L) and upper (6.5-U) (24 x 32 -> 36 x 48 ch) (by adding periscope)
 - total 5000 channels from 5 IRVBs optimized for 3D tomography

